Physical Review B **73** (2006) 125428 (*13 pages*)

# Translational dynamics and friction in double-walled carbon nanotubes

J. Servantie and P. Gaspard
*Center for Nonlinear Phenomena and Complex Systems*
*Université Libre de Bruxelles, Code Postal 231, Campus Plaine, B-1050 Brussels, Belgium*

We report on a study of the translational sliding motion and dynamic friction in systems of double-walled carbon nanotubes using molecular dynamics simulations combined with theoretical analysis. The sliding motion is described by a one-dimensional analytical model which includes the van der Waals force between the nanotubes, a dynamic friction force, and a small Langevin-type fluctuating force. The dynamic friction force is shown to be linear in the velocity over a large domain of initial conditions in armchair-armchair, zigzag-armchair, and zigzag-zigzag double-walled nanotubes. Beyond this domain, evidence is obtained for nonlinear effects which increase friction. In armchair-armchair systems, the dynamic friction is observed to be nonlinearly enhanced by the excitation of internal modes. In the linear domain, the coefficient of proportionality between the dynamic friction force and the velocity is shown to be given by Kirkwood's formula in terms of the force autocorrelation function.

PACS numbers: 68.35.Af;85.35.Kt

## I. INTRODUCTION

Since the experiment of Cumings and Zettl[1] showed the possibility of making nanoscale mechanical devices with multiwalled carbon nanotubes, many papers appeared on the translational motion in these systems. Carbon nanotubes interact by van der Waals forces which keep the nanotubes nested together. Mechanical considerations as well as molecular dynamics simulations have been carried out in double-walled carbon nanotubes (DWNT), showing that oscillations are possible with a frequency larger than gigahertz.[2–4] These oscillations concern the one-dimensional translational motion of the two nanotubes sliding one with respect to the other along their axes. The energy of this one-dimensional motion can be dissipated into the many other degrees of freedom of the nanotubes, resulting in a damping of the mechanical oscillations. This damping is caused by the dynamic friction between both nanotubes. The dynamic friction force against sliding motion is observed to be two orders of magnitude smaller than the van der Waals restoring force. Accordingly, the damping is achieved over long time intervals of the order of hundreds of picoseconds or more[5,6]. Several recent papers have been devoted to the properties of dynamic friction in nanotubes. The role of the commensuration in the corrugation of the force between both nanotubes has been investigated and friction has been expected to be larger in commensurate than incommensurate systems[6–8]. In a recent Letter,[9] it was shown that the commensuration does not lead to significantly increased friction forces while their velocity dependence as well as edge effects play important roles.

The purpose of the present paper is to carry out a systematic study of dynamic friction in carbon nanotubes thanks to the statistical-mechanical method we have described in a previously published Letter.[5] This method is based on earlier work by Jarzynski,[10], Berry and Robbins[11] on dissipation and deterministic friction in finite systems. This method allows us to investigate the dependence of dynamic friction on the relative position and velocity between the nanotubes, as well as on their geometry and, in particular, their commensuration.

The Hamiltonian motion of different types of double-walled carbon nanotubes is simulated by molecular dynamics. The dynamic friction coefficient can be computed by our statistical-mechanical method as well as by direct simulation of the atomic motion. The comparison between the methods allows us to determine the dependence of the dynamic friction force on the relative velocity for different types of double-walled nanotubes. Moreover, the effective potential of the one-dimensional sliding motion is obtained as a function of temperature. Finally, the thermal fluctuations due to the many degrees of freedom of these systems are shown to manifest themselves at long times after the damping of the mechanical oscillations. The overall motion can be modeled by a Langevin stochastic equation describing the nonequilibrium and equilibrium dynamics of the double-walled nanotubes.

The paper is organized as follows. In Section II, the system and its Hamiltonian is defined, the theory of dynamic friction is discussed, and the effective Langevin equation used to model the dynamics is presented. In Section III, the motion is studied at low velocity and analytic solutions of the equations of motion are obtained which allows us to determine the coefficients of dynamic friction directly from the molecular dynamics simulations. This method is applied to different types of double-walled nanotubes in Sec. IV. The dependence of dynamic friction on the relative position and velocity is investigated in Sec. V. Section VI is devoted to the complete model including the Langevin

| DWNT | $N_1$ | $N_2$ | $\mu$ (amu) | $\ell_1$ (Å) | $\ell_2$ (Å) | $d_1$ (Å) | $d_2$ (Å) | $\delta$ (Å) |
|---|---|---|---|---|---|---|---|---|
| (4,4)@(9,9) | 400 | 900 | 3323 | 61.5 | 61.3 | 6.07 | 13.22 | 3.58 |
| (7,0)@(9,9) | 406 | 900 | 3357 | 61.1 | 61.4 | 5.80 | 13.21 | 3.71 |
| (7,0)@(16,0) | 406 | 928 | 3389 | 61.0 | 61.3 | 5.80 | 13.30 | 3.75 |

TABLE I: Parameters of the armchair-armchair (4,4)@(9,9), zigzag-armchair (7,0)@(9,9), and zigzag-zigzag (7,0)@(16,0) DWNTs: $N_a$ are the numbers of carbon atoms, $\mu$ is the relative mass, $\ell_a$ the lengths, $d_a$ the diameters of the inner ($a = 1$) and outer ($a = 2$) tubes, and $\delta = (d_2 - d_1)/2$ the intertube distance. The lengths and diameters are measured at zero temperature and with both nanotubes interacting.

stochastic force which is shown to dominate only at equilibrium. Conclusions are drawn in Sec. VII.

## II. THEORY

### A. The total Hamiltonian

The Hamiltonian of the DWNT system can be written as,

$$H = T^{(1)} + T^{(2)} + V_{\rm TB}^{(1)} + V_{\rm TB}^{(2)} + \sum_{i=1}^{N_1}\sum_{j=1}^{N_2} V_{\rm LJ}\left(\|\mathbf{r}_i^{(1)} - \mathbf{r}_j^{(2)}\|\right) \tag{1}$$

where $T^{(1)}$ and $T^{(2)}$ are respectively the kinetic energies of the inner and outer nanotubes while $V_{\rm TB}^{(1)}$ and $V_{\rm TB}^{(2)}$ are the Tersoff-Brenner potentials of both nanotubes. The positions and momenta of the carbon atoms of both nanotubes are denoted by $\{\mathbf{r}_i^{(a)}\}_{i=1}^{N_a}$ and $\{\mathbf{p}_i^{(a)}\}_{i=1}^{N_a}$ with $a = 1$ (resp. $a = 2$) for the inner (resp. outer) tube. The kinetic energies are given by $T^{(a)} = (1/2m)\sum_{i=1}^{N_a}(\mathbf{p}_i^{(a)})^2$, where $m = 12$ amu is the mass of a carbon atom. The intratube interactions are described by the Brenner potential given by the set of parameters in Table III of Reference[12]. This set reproduces well the G-band peak at 1600 cm$^{-1}$ and the experimental radial breathing mode (RBM) frequencies. We have calculated the RBM frequency for different nanotube diameters and obtained the following factor $\omega_{\rm RBM} = 207/d$ cm$^{-1}$ while the experimental value[13] is $\omega_{\rm RBM} = 224/d$ cm$^{-1}$ ($d$ being the diameter of the nanotube in nm). The intertube potential is modeled by the widely used 6-12 Lennard-Jones potential

$$V_{\rm LJ}(r) = 4\epsilon\left[\left(\frac{\sigma}{r}\right)^{12} - \left(\frac{\sigma}{r}\right)^{6}\right] \tag{2}$$

with $\epsilon = 2.964$ meV and $\sigma = 3.407$ Å, which was successfully used to study $C_{60}$ solids[14] and the sliding of nanotubes on graphite surface[15].[16]

There exist nanotubes of different geometries depending on the way the graphene sheet is rolled into a tube.[13] These geometries are specified by the integers $(n, m)$ with $0 \leq |m| \leq n$. These integers define the chiral vector $n\mathbf{a}_1 + m\mathbf{a}_2$ giving the equator of the nanotube in terms of the lattice vectors $\mathbf{a}_1$ and $\mathbf{a}_2$ of the hexagonal lattice of graphene. The diameter of the nanotube is given by

$$d = \frac{a}{\pi}\sqrt{n^2 + m^2 + n\,m} \tag{3}$$

with $a \simeq 2.5$ Å.[13] The so-called armchair nanotubes correspond to the integers $(n, n)$, the zigzag ones to $(n, 0)$, and the chiral nanotubes to $(n, m)$ with $n \neq m$.[13]

We focus on three similar DWNTs of different geometries, namely, the armchair-armchair (4,4)@(9,9), the zigzag-armchair (7,0)@(9,9), and the zigzag-zigzag (7,0)@(16,0) DWNTs. Their characteristic quantities are given in Table I and two of them are depicted in Fig. 1.

The motion of the atoms in the system is ruled by Hamilton's equations

$$\begin{cases} \frac{d\mathbf{r}_i^{(a)}}{dt} = +\frac{\partial H}{\partial \mathbf{p}_i^{(a)}} \\ \frac{d\mathbf{p}_i^{(a)}}{dt} = -\frac{\partial H}{\partial \mathbf{r}_i^{(a)}} \end{cases} \tag{4}$$

with $i = 1, 2, ..., N_a$ and $a = 1, 2$. The motion conserves the total energy $E = H$, the total linear momentum, as well as the total angular momentum. The phase-space volumes are preserved according to Liouville's theorem.

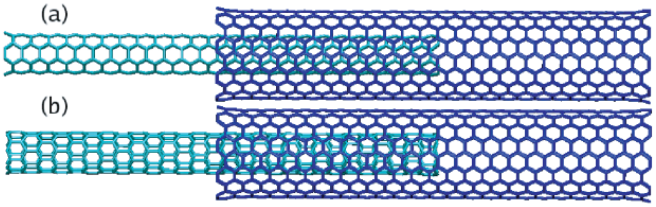


FIG. 1: (color online). (a) The armchair-armchair (4,4)@(9,9) and (b) the zigzag-armchair (7,0)@(9,9) DWNTs.

Hamilton's equations are integrated by a velocity Verlet algorithm with a time step of 2 fs. The total energy was checked to be conserved with a relative error smaller than 0.1%. The initial velocities of the atoms are distributed according to a Maxwell-Boltzmann distribution. Since the initial configuration of the nanotubes is optimized for zero temperature, the total kinetic energy of the initial velocities should take a value twice as large as the value corresponding to the desired temperature. Using the molecular dynamics itself, the initial distribution of velocities is observed to reach the Maxwell-Boltzmann temperature corresponding to the desired temperature in less than 0.5 ps. This provides a convenient method to obtain a system at the desired temperature, without using any algorithm other than the molecular dynamics itself. Furthermore, the total linear momentum is set equal to zero as well as the component of angular momentum along the $z$-axis, in order to avoid a uniform motion of the total center of mass and a global rotation around the axis of the DWNT system.

The dynamics of a complex system such as a DWNT is characterized by different intrinsic time scales:

(1) The correlation time $t_{\rm C}$: This short time is of the order of the vibrational period of the carbon atoms around their equilibrium positions. It can be evaluated in terms of the Debye frequency $\omega_{\rm D}$ as $t_{\rm C} \simeq 2\pi/\omega_{\rm D}$, which is of the order of 50 fs for graphite and carbon nanotubes.[17] The many vibrational modes as well as their anharmonicities contribute to a loss of statistical correlation of typical observables over the correlation time.

(2) The period of oscillations $t_{\rm P}$: This is the main time scale of the DWNT dynamics. It is of the order of 10 ps.

(3) The damping or relaxation time $t_{\rm R}$: It is the time over which the mechanical oscillations are damped. It is of the order of 1 ns and thus a hundred times longer than the period $t_{\rm P}$.

These different characteristic times are therefore ordered as

$$t_{\rm C} \ll t_{\rm P} \ll t_{\rm R} \tag{5}$$

in the DWNT systems which are studied in the present paper.

### B. Effective equation for the relative motion

The description of the translational motion of the nanotubes only retains the relative position $r$ and velocity $v = \dot{r}$ of the nanotubes. This motion concerns the centers of mass of both nanotubes:

$$\mathbf{R}^{(a)} = \frac{1}{N_a} \sum_{i=1}^{N_a} \mathbf{r}_i^{(a)} \tag{6}$$

with $a = 1, 2$. The relative position $r$ is defined as the projection of the vector joining the two centers of mass onto the axis $\mathbf{e}_\parallel(t)$ of the DWNT total system:

$$r(t) \equiv \mathbf{e}_\parallel(t) \cdot \left[ \mathbf{R}^{(2)}(t) - \mathbf{R}^{(1)}(t) \right] \tag{7}$$

The unit vector $\mathbf{e}_\parallel$ is obtained by diagonalizing the inertia tensor

$$I_{\alpha\beta} = m \sum_{a,i} \left( \delta_{\alpha\beta}\, \mathbf{r}_i^{(a)2} - r_{i\alpha}^{(a)}\, r_{i\beta}^{(a)} \right) \tag{8}$$

of the total system and selecting the eigenvector associated with its smallest eigenvalue, which defines the axis of the DWNT. The eigenvector $\mathbf{e}_\parallel$ slightly fluctuates during the time evolution around its initial orientation.

Moreover, the relative mass of the DWNT system is defined by

$$\frac{1}{\mu} \equiv \frac{1}{N_1 m} + \frac{1}{N_2 m} \tag{9}$$

which is given in Table I for the systems we consider.

The relative position $r(t)$ evolves on time scales which are longer than the Debye time scale $t_{\rm C} \sim 50$ fs of the intratube vibrational motion according to Eq. (5). This naturally suggests that the relative position of the nanotubes admits a reduced description in terms of a Newtonian equation of Langevin type:

$$\mu\, \ddot{r} = F_{\rm pot} + F_{\rm frict} + F_{\rm fluct} \tag{10}$$

The first contribution is the force due to the effective potential $V(r)$ of the van der Waals interaction between the two nanotubes:

$$F_{\rm pot} = -\frac{dV(r)}{dr} \tag{11}$$

Since the energy of the one-dimensional sliding motion is dissipated into the other (vibrational) degrees of freedom, there is a dynamic friction force opposed to the motion and which vanishes with the relative velocity $v = \dot{r}$. The dynamic friction force can thus be expanded in powers of the relative velocity as

$$F_{\rm frict} = -\gamma_1 v - \gamma_2 |v| v - \gamma_3 v^3 + \cdots \tag{12}$$

where the coefficients $\gamma_\alpha$ characterize the dynamic friction at different orders in the velocity. According to Eq. (12), the linear dependence on the velocity should be the major contribution to the friction force at low relative velocities $|v| \ll \gamma_1/\gamma_2, \sqrt{\gamma_1/\gamma_3}, ...$ if $\gamma_1 \neq 0$. The friction force would nonlinearly depend on the velocity if $\gamma_1 = 0$ or if the velocity reaches large values during the motion. Moreover, these friction coefficients may have a dependence on the relative position $\gamma_\alpha(r)$. Such dependences on the relative velocity and position are suggested by the study of dynamic friction in the context of Brownian motion, since the pioneering work by Einstein.[18] In 1946, Kirkwood derived a formula giving the friction coefficient $\gamma_1$ in terms of the statistical autocorrelation function of the fluctuating force between the two parts of the total system.[19] In the sixties, Mori,[20] and others developed projection-operator methods to derive generalized Langevin equations and the Kirkwood formula. More recently, friction has been investigated in mesoscopic environments of finite size[21] as well as by molecular dynamics simulations with a finite number of particles.[22,23] Energy dissipation by friction has also been studied in time-dependent driven systems with a multiple-time-scale approach developed by Jarzynski,[10] Berry and Robbins.[11] In these approaches,[10,11,19–23] the relative velocity $v$ can be considered as a small parameter in terms of which the friction force is expanded to obtain the successive friction coefficients $\gamma_\alpha$ in Eq. (12). This is justified as long as the relative velocity is smaller than the ratio of the graphene lattice constant $a \simeq 2.5$ Å over the vibrational correlation time $t_{\rm C} \sim 50$ fs: $v < a/t_{\rm C} \sim 5000$ m/s, which is well satisfied in the systems here studied.

The dependences of the friction force on velocity and position are discussed in Sec. V where we show that dynamic friction is linear in the velocity up to a critical velocity, beyond which the nonlinear dependence on the velocity becomes important. For a friction which is linear in the velocity, the methods[10,11,18–23] of nonequilibrium statistical mechanics lead to a generalized Langevin equation of the form

$$\mu\, \ddot{r} = -\frac{dV(r)}{dr} - \beta \int_0^t dt'\; C(t')\; \dot{r}(t-t') + F_{\rm fluct}(t) \tag{13}$$

with the inverse effective temperature $\beta = 1/(k_{\rm B}T)$. The effective temperature is defined in terms of the microcanonical entropy $S$ by $T^{-1} = \partial S/\partial E$ where $E$ is the total internal energy. The friction kernel $C(t)$ is the force autocorrelation function

$$C(t) = \langle F_{\rm LJ}(t) F_{\rm LJ}(0) \rangle_{E,r} - \langle F_{\rm LJ} \rangle^2_{E,r} \tag{14}$$

where $F_{\rm LJ}$ is the total Lennard-Jones force between the nanotubes and in the direction of their axis. In the projection operator method,[20–23] the force $F_{\rm LJ}(t)$ is projected according to the operator which defines the reduced description of the dynamics. The relation to the actual force available in numerical simulations has been discussed in the literature.[20–23] It is known that the time integral of the autocorrelation function of the actual force decays to zero typically as

$$\int_0^t dt'\; C(t') \simeq \frac{\gamma}{\beta}\, {\rm e}^{-\gamma t/\mu} \tag{15}$$

for $t \gg t_{\rm C}$ and where $\gamma = \gamma_1$ is the friction coefficient.[21–23] The reason is that the force is the time derivative of the momentum. The sliding motion and its damping evolve on time scales $t_{\rm P}$ and $t_{\rm R}$ which are longer than the correlation time $t_{\rm C}$ according to Eq. (5). The time integral (15) reaches its maximum value $\gamma/\beta$ giving the value of the friction coefficient $\gamma$ over a short cutoff time $\tau$ of the order of the correlation time: $\tau \sim t_{\rm C}$. The use of such a cutoff time $\tau$ was proposed by Kirkwood[19] and this procedure provides a reasonable value for the friction coefficient as confirmed by the other methods described in the following section.

On time scales longer than the correlation time $t \gg t_{\rm C}$, the term with the time integral in the generalized Langevin equation (13) tends to a friction force (12) which is linear in the velocity $v = \dot{r}$:

$$\mu\, \ddot{r} = -\frac{dV(r)}{dr} - \gamma\, \dot{r} + F_{\rm fluct}(t) \tag{16}$$

The friction coefficient is given by the Kirkwood formula[5,19]

$$\gamma = \gamma_1 \simeq \beta \int_0^\tau dt\; C(t) \tag{17}$$

in terms of the force autocorrelation function (14). This latter is calculated by statistical average over an ensemble of trajectories for fixed relative position $r$ between the nanotubes. This constraint is enforced by modifying the force on all the atoms of each nanotube according to

$$\mathbf{F}_i^{(a)} \to \mathbf{F}_i^{(a)} - \frac{1}{N_a} \sum_{j=1}^{N_a} \mathbf{F}_j^{(a)} \tag{18}$$

This modification has the required effect of canceling the acceleration of the centers of mass of each nanotube, while conserving the total energy $E$. This method gives the dependence of the friction coefficient on position as discussed in Sec. V where we shall see that this dependence can be neglected in a first approximation. As we have shown elsewhere,[5] the time integral of the autocorrelation function goes as the square of the temperature so that the friction coefficient of DWNT increases linearly with temperature, $\gamma \sim T$, according to Eq. (17). This result has recently been confirmed.[24]

The last contribution $F_{\rm fluct}$ to the force in Eq. (10) is due to the thermal fluctuations caused by the vibrational degrees of freedom of the total system. This fluctuating force becomes dominant for motions of small amplitudes near the statistical equilibrium, as discussed in Sec. VI.

### C. Effective potential between the nanotubes

In our last study,[5] we approximated the total Lennard-Jones potential by a harmonic potential. This approximation is only valid if the distance $r$ between the centers of mass is sufficiently small. For motions of larger amplitude, the potential becomes linear in the distance as seen in Fig. 2 where we depict the total intertube potential energy calculated for different temperatures and DWNTs.

We see that the following potential is a very good approximation,

$$V(r) \simeq \begin{cases} F\sqrt{r^2+\ell^2} - F\sqrt{L^2+\ell^2}\;, & \text{for} \quad |r| < L \\ 0\;, & \text{for} \quad |r| > L \end{cases} \tag{19}$$

where $L$ is the length of the two nanotubes. For separations $|r|$ smaller than the distance $\ell \simeq 0.2 - 0.3$ nm, the potential is essentially harmonic

$$V(r) \simeq \frac{k}{2}\, r^2 - F(L-\ell) \qquad \text{for} \quad |r| < \ell \tag{20}$$

with $k = F/\ell$, which is the case for small nanotubes. If the nanotubes are long enough, typically larger than 2 nm, the intertube potential energy grows linearly with the number of van der Waals bonds between the nanotubes. This number is proportional to the length $L-|r|$ of the segment where the nanotubes overlap. For large amplitude motions, the harmonic part of the potential becomes negligible in comparison with the linear part. The dynamics is thus mainly described by the linear part. In such circumstances, we can use the simplified V-shaped potential:

$$V(r) \simeq F|r| - FL \qquad \text{for} \quad \ell < |r| < L \tag{21}$$

$F$ is the van der Waals restoring force which does not depend on the length of the DWNT but only on the radii of the two interacting nanotubes.

The dependence of the van der Waals restoring force on temperature is also depicted in Fig. 2. We perform constrained molecular dynamics simulations to calculate the average potential at non-zero temperatures and the restoring force for a given separation between the centers of mass. Because of the thermal expansion, the radii of the nanotubes increase as well as their radial separation, thus decreasing the total interaction energy. The interesting result is that the van der Waals restoring force decreases linearly with temperature with a slope of 0.0706 pN/K (resp. 0.0798 pN/K) for the armchair-armchair (resp. zigzag-armchair) system, as seen in the insets of Fig. 2.

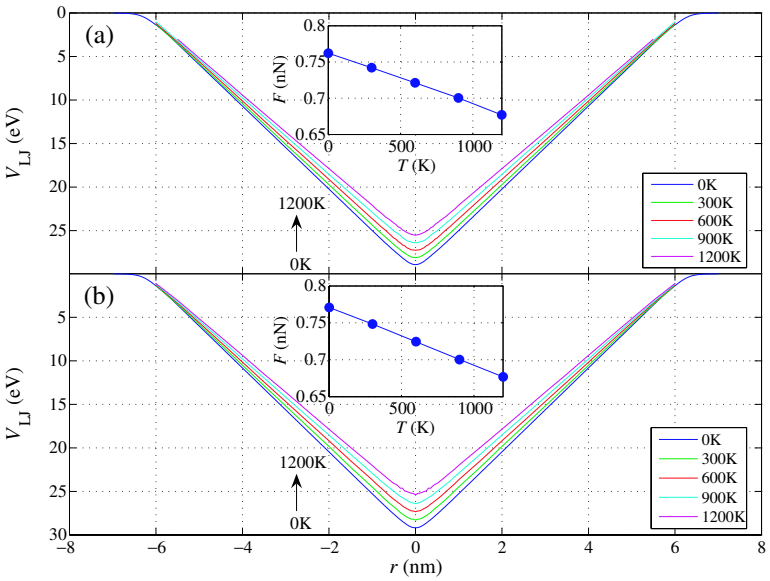


FIG. 2: (color online). Plot of the total Lennard-Jones potential energy $V = V_{\rm LJ}$ as a function of the distance $r$ between the centers of mass for (a) the armchair-armchair (4,4)@(9,9) and (b) the zigzag-armchair (7,0)@(9,9) DWNTs. Both double-walled nanotubes are of length 6.1 nm. The insets depict the force versus the temperature.

## III. LOW-VELOCITY MOTION

In this section, we consider the motion at low velocity starting from an initial configuration where the inner tube is extracted from the outer tube by a separation $\ell < r_0 < L$. We here suppose that dynamic friction is linear in the velocity while the motion is sufficiently far from equilibrium to neglect the Langevin stochastic force. The motion can thus be obtained by solving the following Newton equation,

$$\mu\,\ddot{r} = -\frac{dV(r)}{dr} - \gamma\,\dot{r} \tag{22}$$

where $V(r)$ is the V-shaped potential (21), $\gamma$ is the friction coefficient, and $\mu$ the relative mass (9). The solution of Eq. (22) for $r > 0$ is

$$r(t) \;=\; r(0) + v(0)\frac{\mu}{\gamma}\left(1 - {\rm e}^{-\gamma t/\mu}\right) + \frac{\mu F}{\gamma^2}\left(1 - \frac{\gamma}{\mu}\,t - {\rm e}^{-\gamma t/\mu}\right) \tag{23}$$

$$v(t) \;=\; v(0)\,{\rm e}^{-\gamma t/\mu} - \frac{F}{\gamma}\left(1 - {\rm e}^{-\gamma t/\mu}\right) \tag{24}$$

The solution for $r < 0$ is obtained by the substitution $F \to -F$. The calculation we describe is schematically depicted in Fig. 3. Without damping, the position follows successive arcs of parabola connected with each other at $r = 0$. The amplitude of these oscillations is progressively damped because of friction. Accordingly, the maximum extension decreases by $\Delta R$ at each oscillation. Our goal is to calculate the damping $\Delta R$ and find a continuous function describing the succession of parabolas.

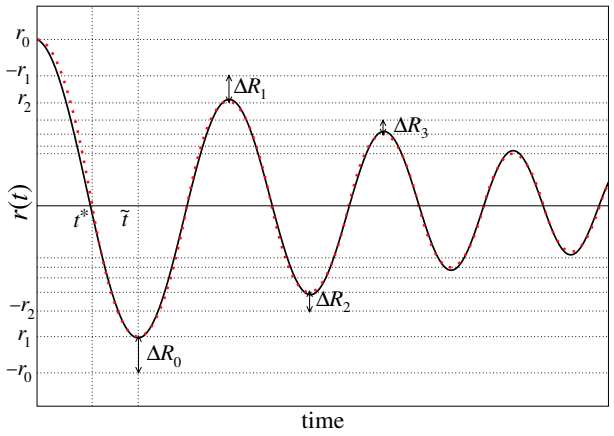


FIG. 3: (color online). Schematic representation of a trajectory of Eq. (22), defining the notations used in the text (solid line). The dotted line is the approximation given by Eq. (48).

After the initial extraction of the inner tube with respect to the outer one, the motion starts from the initial condition $r(0) = r_0$ and $v(0) = 0$.

The time when the distance between the centers of mass reaches zero is denoted by $t^*$. This time is the root of $r(t^*) = 0$ using the solution of Eq. (23) with the aforementioned initial conditions:

$$\frac{\gamma}{\mu}\, t^* + \mathrm{e}^{-\gamma t^*/\mu} = \frac{\gamma^2 r_0}{\mu F} + 1 \tag{25}$$

The implicit equation (25) can be written as

$$\eta + \mathrm{e}^{-\eta} = \xi \tag{26}$$

in terms of the variables $\eta = \gamma t^*/\mu$ and $\xi = [\gamma^2 r_0/(\mu F)] + 1$. Equation (26) admits a solution in terms of the Lambert $W$ function[25] defined as the root of

$$W(z)\, \mathrm{e}^{W(z)} = z \tag{27}$$

Indeed, Eq. (26) can be rewritten as

$$(\eta - \xi)\, \mathrm{e}^{\eta - \xi} + \mathrm{e}^{-\xi} = 0 \tag{28}$$

and we get

$$W\, \mathrm{e}^{W} = -\mathrm{e}^{-\xi} \tag{29}$$

by defining $W = \eta - \xi$. Accordingly, we find that

$$\eta = \xi + W(-\mathrm{e}^{-\xi}) \tag{30}$$

Since the friction coefficient is small ($\gamma < 10$ amu/ps) and the relative mass is large ($\mu > 1000$ amu), $\xi \to 1$, we can thus expand the Lambert function as

$$\eta = \sqrt{2(\xi - 1)} + \frac{1}{3}(\xi - 1) + O\left((\xi - 1)^{3/2}\right) \tag{31}$$

Hence, $t^*$ is given by

$$t^* = \sqrt{\frac{2\mu r_0}{F}} + \frac{\gamma r_0}{3F} + O\left(\frac{\gamma^2 r_0^{3/2}}{\mu^{1/2} F^{3/2}}\right) \tag{32}$$

The period can thus be approximated by

$$P_0 \simeq 4\left(\sqrt{\frac{2\mu r_0}{F}} + \frac{\gamma r_0}{3F}\right) \tag{33}$$

This relation contains a first-order correction in the friction with respect to the period derived by Zheng and Jiang.[2,3] The maximum velocity which is reached at time $t^*$ is given by

$$v_{\max} = v(t^*) = -\sqrt{\frac{2Fr_0}{\mu}} + \frac{2\gamma}{3\mu} r_0 + O\left(\frac{\gamma^2 r_0^{3/2}}{\mu^{3/2} F^{1/2}}\right) \tag{34}$$

Knowing the time $t^*$ when $r(t^*) = 0$, we can look for the solution in the region $r < 0$ by imposing continuity on the position and velocity. We get

$$r(t) = \frac{\mu F}{\gamma^2}\left(2 - \mathrm{e}^{-\gamma t^*/\mu}\right)\left(\mathrm{e}^{-\gamma(t-t^*)/\mu} - 1\right) + \frac{F}{\gamma}(t - t^*) \tag{35}$$

$$v(t) = -\frac{F}{\gamma}\left(2 - \mathrm{e}^{-\gamma t^*/\mu}\right)\mathrm{e}^{-\gamma(t-t^*)/\mu} + \frac{F}{\gamma} \tag{36}$$

Now, the time $\tilde{t}$ when the velocity vanishes again is given by

$$\tilde{t} = t^* + \frac{\mu}{\gamma}\ln\left(2 - \mathrm{e}^{-\gamma t^*/\mu}\right) \tag{37}$$

Replacing the time $\tilde{t}$ in the equation (35) for position, we obtain the first minimum of the position after half a period as

$$r(\tilde{t}) = \frac{\mu F}{\gamma^2}\left[-1 + \mathrm{e}^{-\gamma t^*/\mu} + \ln\left(2 - \mathrm{e}^{-\gamma t^*/\mu}\right)\right] \tag{38}$$

Substituting the exact expression of $t^*$ and expanding for $\xi \to 1$ finally gives

$$r(\tilde{t}) = -r_0 + \frac{4}{3} r_0\left(\sqrt{\frac{2\gamma^2 r_0}{\mu F}} - \frac{2\gamma^2 r_0}{\mu F}\right) + O\left(\frac{\gamma^3 r_0^{5/2}}{\mu^{3/2} F^{3/2}}\right) \tag{39}$$

The second term in the parentheses is much smaller than the first one since it goes as $\gamma^2/\mu$ so that we can write

$$r_{n+1} \simeq -r_n + \frac{4}{3} r_n \sqrt{\frac{2\gamma^2 |r_n|}{\mu F}} \tag{40}$$

where $r_n$ denote the extrema at each half period. The equation for the absolute value of the distances between the centers of mass is

$$|r_{n+1}| \simeq |r_n| - \frac{4}{3}|r_n|\sqrt{\frac{2\gamma^2 |r_n|}{\mu F}} \tag{41}$$

hence the damping at the $n^{\text{th}}$ half period is given by

$$\Delta R_n \simeq -\frac{4}{3} R_n \sqrt{\frac{2\gamma^2 R_n}{\mu F}} \tag{42}$$

with $R \equiv |r|$. The time for going from one extremum $R_n$ to the next $R_{n+1}$ is approximately

$$\Delta t \simeq 2\sqrt{\frac{2\mu R_n}{F}} \tag{43}$$

Since the damping is small in the limit $\mu \to \infty$, the period of oscillation is short with respect to the relaxation time and we therefore obtain

$$\frac{dR}{dt} \simeq \frac{\Delta R}{\Delta t} \simeq -\frac{2\gamma}{3\mu} R \tag{44}$$

| quantity | damping rate | harmonic potential | V-shaped potential |
|---|---|---|---|
| position | $\Gamma_R$ | $\frac{\gamma}{2\mu}$ | $\frac{2\gamma}{3\mu}$ |
| energy | $\Gamma_E$ | $\frac{\gamma}{\mu}$ | $\frac{2\gamma}{3\mu}$ |
| period | $\Gamma_P$ | 0 | $\frac{\gamma}{3\mu}$ |

TABLE II: Damping rates of the position, the energy, and the period of the mechanical oscillations in the harmonic and V-shaped potentials.

hence the maximum separation between the centers of mass decays as

$$R(t) = R_0 \ \exp\left(-\frac{2\gamma}{3\mu}t\right) = R_0 \ \exp\left(-\Gamma_R t\right) \tag{45}$$

Since the energy at the extrema is only equal to the potential energy, we get

$$E(t) = E_0 \ \exp\left(-\frac{2\gamma}{3\mu}t\right) = E_0 \ \exp\left(-\Gamma_E t\right) \tag{46}$$

for the energy $E = (1/2)\mu\dot{r}^2 + V(r)$ of the one-dimensional sliding motion. Finally, the period can be approximated by

$$P(t) = P_0 \ \exp\left(-\frac{\gamma}{3\mu}t\right) = P_0 \ \exp\left(-\Gamma_P t\right) \tag{47}$$

where the initial period $P_0$ is given by Eq. (33). Since we know the damping of the amplitude and the period as a function of time one can approximate the oscillating function of time by

$$r(t) \simeq r_0 \cos\left[\omega(t)t\right] \exp\left(-\Gamma_R t\right) \tag{48}$$

where $\omega(t) = 2\pi/P(t)$ is the frequency defined in terms of the period (47).

For long times or short nanotubes, the dynamics is governed by the harmonic potential, in which case the period is isochronous and the damping rates of position and energy are no longer equal but in the ratio 1 : 2 as described in our Letter.[5] The different damping rates are given in Table II. Since the motion of the DWNTs can be simulated by molecular dynamics, the friction coefficient can be determined from the damping rates of Table II in the different regimes.

## IV. ANALYSIS OF TYPICAL SYSTEMS

In the present section, we describe the motion of the armchair-armchair and zigzag-armchair DWNTs of Table I, as simulated by molecular dynamics. The motion is simulated for an initial extraction of 3 nm and a temperature of 300 K. First, we study the energy of the one-dimensional sliding motion which is defined as the sum of the kinetic energies of mass centers and of the total Lennard-Jones potential. This energy differs from the total energy by the energy of all the other degrees of freedom so that we expect energy dissipation to occur. We observe in Fig. 4 the dissipation of the energy of the one-dimensional sliding motion from the initial energy $Fr_0$. This dissipation results into the damping of the amplitudes of the mechanical oscillations as shown in Fig. 5, which depicts the successive extrema of the distance between the centers of mass as a continuous function (so that the oscillations are not visible in this figure). The successive periods of oscillation are depicted in Fig. 6. In Figs. 4-6, the dashed lines are exponential fits to the results of the molecular dynamics simulations.

We see that the relaxation rate changes after approximately one nanosecond when the system approaches equilibrium and the sliding motion becomes exclusively restricted to the harmonic region of the intertube van der Waals potential. In this small amplitude regime, the motion is isochronous as seen in Fig. 6. Simultaneously, the damping rates of energy and position change to the new values characteristic of the harmonic potential given in Table II.

In the initial large amplitude regime, the relaxation rates are characteristic of the V-shaped potential. Indeed, we give in Table III the relaxation rates of the fits for Figs. 4-6 and we observe that the relations $\Gamma_E = \Gamma_R = 2\Gamma_P$ are verified as it should for a damped sliding motion in the V-shaped potential. Using Eqs. (45), (46), and (47), we find the friction coefficients for both systems to be approximately $\gamma_{\rm aa} = 6.1$ amu/ps for the armchair-armchair system and $\gamma_{\rm za} = 5.7$ amu/ps for the zigzag-armchair one. Knowing the friction coefficient, one can calculate the dynamic

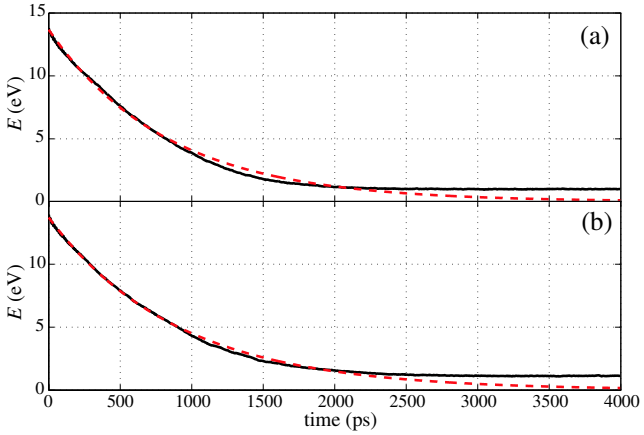


FIG. 4: (color online). Evolution of the sliding energy for (a) the armchair-armchair (4,4)@(9,9) and (b) the zigzag-armchair (7,0)@(9,9) DWNTs.

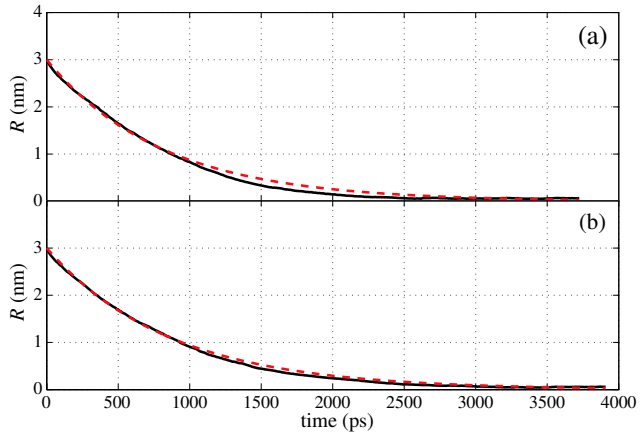


FIG. 5: (color online). Evolution of the distance for (a) the armchair-armchair (4,4)@(9,9) and (b) the zigzag-armchair (7,0)@(9,9) DWNTs.

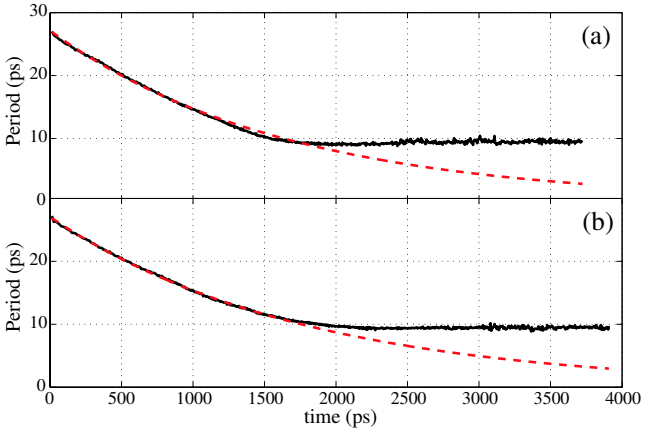


FIG. 6: (color online). Evolution of the period for (a) the armchair-armchair (4,4)@(9,9) and (b) the zigzag-armchair (7,0)@(9,9) DWNTs.

| DWNT | $\Gamma_E$(1/ns) | $\Gamma_R$(1/ns) | $\Gamma_P$(1/ns) |
|---|---|---|---|
| (4,4)@(9,9) | 1.21 | 1.24 | 0.612 |
| (7,0)@(9,9) | 1.11 | 1.15 | 0.565 |

TABLE III: Relaxation rates of the energy, position and period in the large amplitude regime where the intertube potential is well approximated by the V-shaped potential (21).

friction force $f_{\rm k} = |F_{\rm frict}| = \gamma v$. During the first period, the velocity varies linearly between zero and 840 m/s for both systems hence the maximum dynamic friction force is $f_{\rm k,aa} = 8.50$ pN (6.54 fN/atom) for the armchair-armchair system and $f_{\rm k,za} = 7.95$ pN (6.09 fN/atom) for the zigzag-armchair one.

In the harmonic regime near equilibrium, the period of the oscillations can be directly calculated from the harmonic oscillator frequency $\omega = \sqrt{k/\mu}$ where the spring constant can be found from the potentials in Fig. 2 [see Eq. (20)]. We find that the spring constant of the armchair-armchair system is $k_{\rm aa} = 2.53$ N/m and $k_{\rm za} = 2.84$ N/m for the zigzag-armchair one. We thus find an equilibrium period of $P_{\rm aa} = 9.28$ ps for the armchair-armchair system and $P_{\rm za} = 8.80$ ps for the zigzag-armchair one, in agreement with the periods observed in Fig. 6, given that the system heats up because of energy dissipation. The temperature at the end of simulation is equal to $T = T_0 + Fr_0/(3Nk_{\rm B}) = 338\,{\rm K}$ and thus higher than the initial temperature $T_0 = 300\,{\rm K}$.

## V. DEPENDENCE OF FRICTION ON RELATIVE POSITION AND VELOCITY

The purpose of the present section is to discuss the assumptions of the model used in Secs. III and IV that the friction is linear in the velocity with a friction coefficient independent of the relative position between the nanotubes. For this purpose, we investigate the dependences of friction on the relative position and velocity and set up the limits of validity of the previous model.

### A. Dependence of friction on velocity

Concerning the dependence on the relative velocity $v$, we have mentioned with Eq. (12) that friction could become nonlinear in the velocity if this latter increases. Such nonlinearities can be detected numerically by considering the dependence of the damping $\Delta R$ of the amplitude of an oscillation on the initial position $r_0$ (see Fig. 3). In Sec. III, we have shown that the damping of the amplitude over a half period is given by the following relation in the case of linear friction,

$$\Delta R = \frac{4}{3}\sqrt{\frac{2}{\mu F}}\,\gamma\, r_0^{3/2} \tag{49}$$

[see Eq. (42)]. Using the same reasoning as we described in Sec. III but now for a nonlinear dependence on the velocity, we get that the damping of the position over a half period scales as follows with the initial position $r_0$:

$$|F_{\rm frict}| \propto |v|^\alpha \qquad \text{implies} \qquad \Delta R \propto r_0^{(\alpha+2)/2} \tag{50}$$

This result is obtained by supposing the friction force as a perturbation on the dissipationless motion of the conservative one-dimensional oscillator. Neglecting the fluctuations, its energy $E = (1/2)\mu\dot{r}^2 + V(r)$ decreases according to $\dot{E} = \dot{r}F_{\rm frict}$, which can be integrated over time using the dissipationless solution in the right-hand side to get Eq. (50). Hence, the dependence of $\Delta R$ on the initial condition $r_0$ allows us to verify the validity of the linear friction and also provides another way of calculating the friction coefficient of the system. The maximum velocity (34) reached during the half period is depicted as a function of the initial position $r_0$ in Fig. 8.

We represent in Fig. 7 the damping $\Delta R$ of the amplitude of a half oscillation versus the initial separation $r_0$ at the temperature of 300 K for the three systems of Table I. First, we notice the damping has the dependence (49) expected for a friction linear in the velocity up to a separation of the centers of mass, which is larger than half the lengths of the nanotubes in all the cases and reaches up to 90% of their lengths in the zigzag-armchair and zigzag-zigzag DWNTs. This confirms the validity of the assumption of a linear friction for low enough velocity. However, we observe a larger dynamic friction which can be interpreted as due to nonlinear effects according to Eq. (50).

In the zigzag-armchair and zigzag-zigzag DWNTs, the deviations with respect to a friction with a linear dependence on the velocity show up at very large extraction of the nanotubes beyond 90% of their length. At such very large

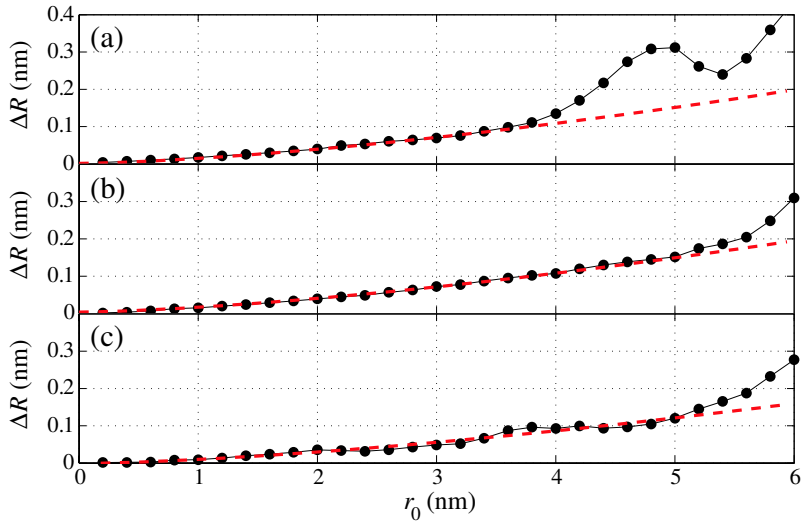


FIG. 7: (color online). Damping during the first half period for (a) the armchair-armchair (4,4)@(9,9) DWNT, (b) the zigzag-armchair (7,0)@(9,9) DWNT, and (c) the zigzag-zigzag (7,0)@(16,0) DWNT. The dots are the results of the simulations and the dashed line a plot using Eq. (49).

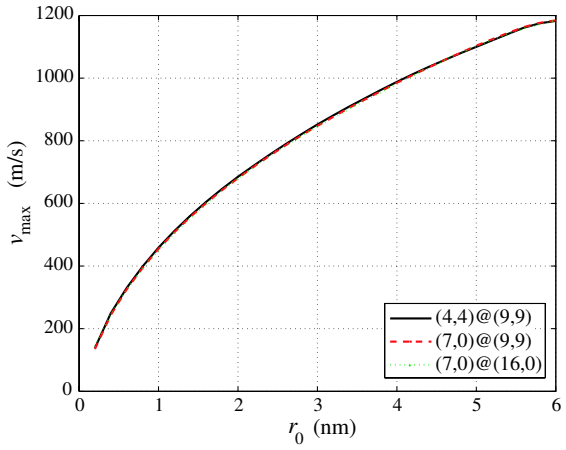


FIG. 8: (color online). The maximum velocity $v_{\max}$ versus the initial extraction $r_0$ for the DWNTs of Fig. 7.

extractions, the dynamics and the friction mainly occur at the edges of the nanotubes, which can explain that the friction becomes nonlinear in the velocity. Similar observations and conclusions have been reported for zigzag-zigzag and zigzag-chiral DWNTs by Tangney et al..[9]

In the armchair-armchair DWNTs, a further mechanism of friction appears to be present. Indeed, the validity of the linear dependence on the velocity is observed to be limited to extraction smaller than $r_0 = 4$ nm in the armchair-armchair (4,4)@(9,9) DWNT, which represents only 65% of the complete extraction. Beyond, the damping becomes larger than expected for linear friction, which indicates that a nonlinear dependence on velocity sets in. The damping increases up to a maximum at $r_0 \simeq 5$ nm corresponding to the critical velocity of 1090 m/s and decreases for larger extractions, in a behavior typical of a resonance. This enhancement of the friction is related to fast variations of the van der Waals restoring force on a time scale of the order of the picosecond. These excitations occur just after the kick undergone by the system when the mean restoring force changes its sign at $r = 0$ during every period. The simulations suggest that radial breathing modes or the bending modes of vibrations of the nanotubes are excited at the kicks. These modes have periods of the order of the picosecond. The excitation of such internal modes explains that energy dissipation is enhanced, which increases the damping $\Delta R$ of the amplitude. Such internal modes may have a frequency varying when the inner and outer tubes telescope each other as observed in the fast variations of

| DWNT | $N_1$ | $N_2$ | $\mu$ (amu) | $\ell_1$ (Å) | $\ell_2$ (Å) | $d_1$ (Å) | $d_2$ (Å) | $\delta$ (Å) |
|---|---|---|---|---|---|---|---|---|
| (4,4)@(9,9) | 400 | 900 | 3323 | 61.5 | 61.3 | 6.07 | 13.22 | 3.58 |
| (5,5)@(10,10) | 500 | 1000 | 4000 | 61.4 | 61.3 | 7.45 | 14.67 | 3.61 |
| (6,6)@(11,11) | 600 | 1100 | 4658 | 61.3 | 61.3 | 8.96 | 16.09 | 3.57 |
| (7,7)@(12,12) | 700 | 1200 | 5305 | 61.3 | 61.3 | 10.36 | 17.53 | 3.59 |
| (8,8)@(13,13) | 800 | 1300 | 5943 | 61.3 | 61.3 | 11.84 | 18.95 | 3.56 |
| (9,9)@(14,14) | 900 | 1400 | 6574 | 61.3 | 61.3 | 13.24 | 20.38 | 3.57 |
| (10,10)@(15,15) | 1000 | 1500 | 7200 | 61.3 | 61.3 | 14.71 | 21.80 | 3.55 |

TABLE IV: Parameters of the armchair-armchair DWNTs of Fig. 9: $N_a$ are the numbers of carbon atoms, $\mu$ is the relative mass $\ell_a$ the lengths, $d_a$ the diameters of the inner ($a = 1$) and outer ($a = 2$) tubes, and $\delta = (d_2 - d_1)/2$ the intertube distance. The lengths and diameters are measured at zero temperature and with both nanotubes interacting.

the van der Waals restoring force after each kick in the armchair-armchair DWNT.

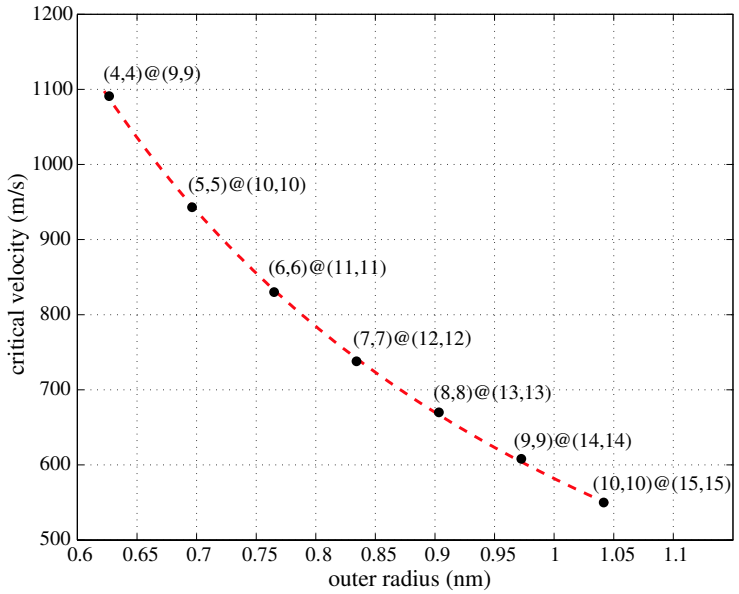


FIG. 9: (color online). Critical velocity as a function of the radius of the outer tube for several armchair-armchair DWNTs. The dashed line is a fit to a power law of exponent $-1.34 \pm 0.02$.

We have studied the critical velocity which marks the resonant maximum of the damping $\Delta R$ in different armchair-armchair DWNTs (see Fig. 9 and Table. IV). First of all, the critical velocity decreases too slowly with temperature (less than 2% of difference between 300 K and 100 K) to be directly related to the average thermal velocity of the carbon atoms. Moreover, the critical velocity is one order of magnitude smaller than the velocity of the three phonon modes. Our calculations gave approximately 8 km/s for the transverse acoustic mode, 11 km/s for the twisting acoustic mode and 18 km/s for the longitudinal acoustic mode. Therefore, the sound velocities are much higher than the possible sliding velocities. The important observation is that the critical velocity significantly decreases as the radii of the nanotubes increase, although it does not depend on their length. The critical velocity is depicted as a function of the radius of the outer tube in Fig. 9. The data can be fitted with a power law of exponent $-1.34 \pm 0.02$. This behavior is reminiscent of the dependence of the frequency $\omega_{\mathrm{RBM}}$ of the radial breathing modes with the nanotube diameters although the exponent is different (see Subsec. II A).[13] This result again suggests that the mechanism leading to the nonlinearities in the friction involves the breathing motion of the nanotubes. We notice that the initial position $r_0$ corresponding to the critical velocity (see Fig. 8) also decreases with the radii in the armchair-armchair DWNTs.

### B. Dependence of friction on position

In the domain of validity of a friction linear in the velocity, we may wonder how the friction coefficient $\gamma$ depends on the relative position $r$ separating the centers of mass of the nanotubes. With such a dependence, the friction force would depend on both the velocity and the position as $F_{\rm frict} = -\gamma(r)v$. The low-velocity model of Sec. III does not assume such a dependence but the Kirkwood formula (17) provides a way to determine the friction coefficient as a function of the relative position. Indeed, the force autocorrelation function in Eq. (14) is averaged while keeping fixed the separation $r$ between the centers of mass. This can be carried out by constrained molecular dynamics simulations as explained in Sec. II. The so-computed force autocorrelation function typically decays to small values over a time of the order of the correlation time $t_{\rm C} \sim 50$ fs. The force autocorrelation function is integrated in time up to the cutoff time $\tau$ to give the friction coefficient according to Kirkwood's formula (17). The cutoff time is here taken when the time integral reaches its first maximum, which corresponds in our system to reaching the plateau value.[21–23]

The resulting friction coefficient is depicted as a function of the relative position in Fig. 10 for the armchair-armchair and zigzag-armchair DWNTs. We observe that this friction coefficient does not depend much on the relative position and its mean value is in agreement with the values of about 6 amu/ps obtained in Sec. IV by the other method. Besides, we notice a dependence on position, in particular, for small extractions when the system moves in the harmonic region where the van der Waals intertube force changes its sign. This important variation in the intertube force can affect not only its mean value but also its correlation function and leads to more important friction in this region. Moreover, we also observe that, for larger extractions, the friction coefficient is approximately constant for the armchair-armchair system albeit it slowly decreases for the zigzag-armchair one.

Such dependences of the friction coefficient on position could be modeled as explained here above but they would not affect the sliding motion in a very important way. The reason is that friction significantly affects the amplitudes of the oscillations only over the relaxation time $t_{\rm R} \sim 1000$ ps, which is much longer than the oscillation period $t_{\rm P} \sim 10$ ps. Therefore, only a spatial average of the friction coefficient $\gamma = \langle \gamma(r) \rangle$ matters for the damping of the oscillations. These results therefore justify the use of a friction coefficient which is independent of the position for a good first approximation of the sliding motion.

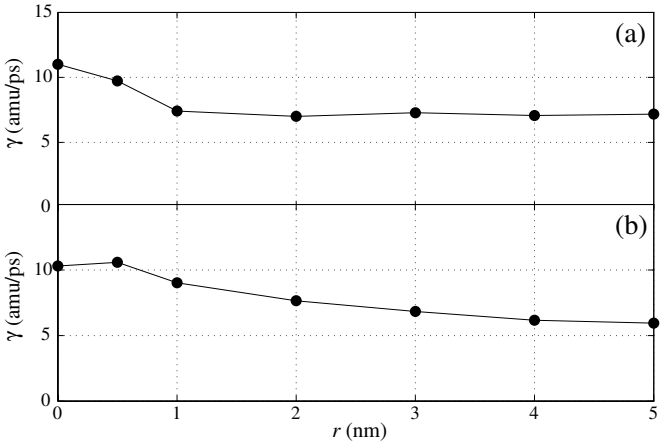


FIG. 10: Friction coefficient calculated by the Kirkwood formula (17) versus the position $r$ for: (a) the armchair-armchair (4,4)@(9,9) and (b) the zigzag-armchair (7,0)@(9,9) DWNTs.

## VI. EQUILIBRIUM FLUCTUATING DYNAMICS

After the damping of the large amplitude oscillations, the dynamics reaches an equilibrium regime near the bottom of the potential. Since total energy is conserved, energy can be transferred between the one-dimensional sliding motion and the many other degrees of freedom. This induces thermal fluctuations which manifest themselves in the equilibrium regime (see Fig. 11). These fluctuations are negligible during the large amplitude oscillations because the van der Waals restoring force and the friction force dominate the force due to the fluctuations. Accordingly, the model should be completed by adding a fluctuating force, leading to the Langevin equation (16). For the modeling of the dynamics over time scales longer than the short correlation time $t_{\rm C}$, this fluctuating force can be taken as a

Gaussian white noise satisfying:

$$\langle F_{\rm fluct}(t)\rangle = 0 \tag{51}$$

$$\langle F_{\rm fluct}(t)F_{\rm fluct}(t')\rangle = 2\,\gamma\,k_{\rm B}T\delta(t-t') \tag{52}$$

in consistency with Kirkwood formula (17) for $|t-t'| \gg t_{\rm C}$.

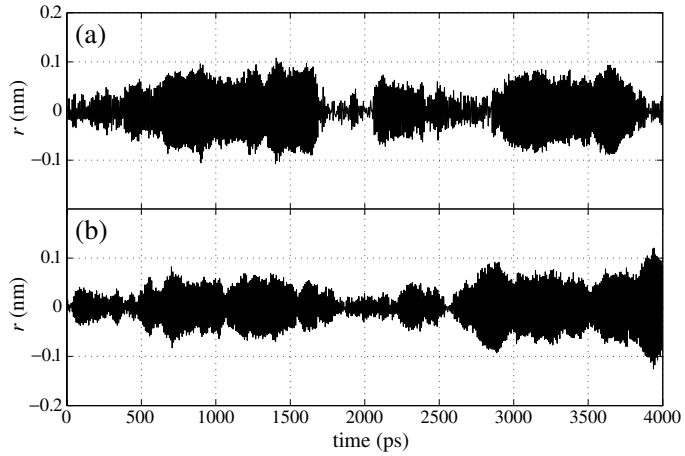


FIG. 11: Equilibrium fluctuating oscillations for (a) the armchair-armchair (4,4)@(9,9) and (b) the zigzag-armchair (7,0)@(9,9) DWNTs.

The probability density $\rho(r,v;t)$ to find the system in the relative position $r$ and velocity $v$ at time $t$ is ruled by the Fokker-Planck master equation associated with the Langevin stochastic equation (16):

$$\frac{\partial\rho}{\partial t} = -v\,\frac{\partial\rho}{\partial r} + \frac{\partial}{\partial v}\left[\frac{1}{\mu}\left(\frac{dV}{dr}+\gamma v\right)\rho\right] + \frac{\gamma k_{\rm B}T}{\mu^2}\frac{\partial^2\rho}{\partial v^2} \tag{53}$$

The stationary solution of this equation is the equilibrium distribution:

$$\rho_{\rm eq}(r,v) = \frac{1}{Z}\exp\left[-\frac{1}{k_{\rm B}T}\left(\frac{1}{2}mv^2+V(r)\right)\right] \tag{54}$$

Near its bottom, the potential can be approximated by the harmonic potential (20) so that the Langevin stochastic equation takes the simpler form

$$\mu\ddot{r} = -kr - \gamma\dot{r} - F_{\rm fluct}(t) \tag{55}$$

with the spring constant $k = F/\ell$. In this case, the variance of the position calculated from the equilibrium distribution (54) with the potential (20) is given by[26]

$$\sigma^2 = \langle r^2\rangle = \frac{k_{\rm B}T}{k} \tag{56}$$

Hence the knowledge of the intertube interaction potential allows us to calculate the standard deviation $\sigma$ and, vice versa, the knowledge of the standard deviation should give the spring constant in the harmonic region.

In order to study the fluctuations in the equilibrium regime, we depict in Fig. 11 the relative position between the nanotubes for the armchair-armchair and zigzag-armchair DWNTs here studied. The initial conditions are chosen such as the distance between the centers of mass is zero and the temperature 300 K. We can calculate the spring constants of both systems at 300 K from the potentials in Fig. 2. The spring constant is $k_{\rm aa} = 2.53$ N/m for the armchair-armchair system and $k_{\rm za} = 2.84$ N/m for the zigzag-armchair one. Having the spring constants, one can directly calculate the standard deviations with Eq. (55) to get $\sigma_{\rm aa} = 0.405$ Å and $\sigma_{\rm za} = 0.382$ Å. The molecular dynamics simulations give the standard deviations $\sigma_{\rm aa} = 0.396$ Å and $\sigma_{\rm za} = 0.360$ Å, respectively. We can thus conclude that the Langevin equation with the harmonic potential reproduces well the translational motion at equilibrium. We notice that the motion due to the thermal fluctuations remains of very small amplitudes of less than 0.1 nm in the relative position. Therefore, the thermal fluctuations are negligible for the large amplitude motion just after an extraction of several nanometers.

## VII. CONCLUSIONS

In the present paper, we have studied the dynamic friction of the sliding motion between two telescoping carbon nanotubes by molecular dynamics simulations combined with a theoretical analysis. The study has been carried out at the ambient temperature of 300 K. For an isolated system of uncapped DWNT, the sliding motion presents mechanical oscillations which are slowly damped because of dynamic friction. The intratube carbon-carbon interaction is described by a Tersoff-Brenner potential and the intertube van der Waals interaction by a Lennard-Jones potential.

The sliding motion takes place in the van der Waals energy potential of the intertube interaction. For the large nanotubes we here study, this potential has the shape of a V with a piecewise constant restoring force. In such an anharmonic potential, the period of the oscillations depends on the initial position and we have carried out in detail the analysis of this motion using a one-degree-of-freedom mechanical model which includes the van der Waals restoring force, the friction force, as well as a Langevin-type fluctuating force. The model has been validated by comparison with molecular dynamics simulations.

Dynamic friction dissipates energy from the one-dimensional sliding motion to the many other vibrational degrees of both nanotubes. The energy dissipation drives the system toward a microcanonical thermodynamic equilibrium where the thermal fluctuations continue to activate irregularly the one-dimensional sliding motion, as it is the case in Brownian motion. However, these fluctuations are of very small amplitudes smaller than 0.1 nm and are negligible during the large amplitude motion following an extraction of the inner tube out of the outer tube by several nanometers. Dynamic friction has the effect of damping the amplitudes of the oscillations which provides a method to determine the properties of dynamic friction.

The friction force is expected to vanish with the relative velocity of the motion of one nanotube with respect to the other. For low enough velocity, a dependence which is linear in the velocity should dominate, but nonlinear terms become important at higher velocity. The question of this dependence of dynamic friction on velocity has been investigated in detail by measuring the damping of the oscillation amplitude over a half period. The larger the initial extraction of one nanotube with respect to the other, the higher the velocity in the middle of the half period and the higher the damping caused by dynamic friction. Thanks to this method, we have shown that the friction force remains linear in the velocity up to critical velocities of several hundreds of meters per second.

In this linear domain, the coefficient of proportionality between the friction force and the velocity has been studied by two methods which give consistent values. The first method is the one mentioned here above, while the second method is based on nonequilibrium statistical mechanics.[10,11,19–23,26] The theory of friction has been developed since a pioneering work by Kirkwood[19] who showed that the friction coefficient is given in terms of the time integral of the force autocorrelation function. As described in our previous Letter,[5] Kirkwood's formula can be applied to friction in DWNTs. This second method allows us to investigate the dependence of the friction coefficient on the relative position of both nanotubes. It is observed that this dependence is relatively small, which justifies the use of a constant coefficient. Both methods give consistent values for the coefficient $\gamma$ of dynamic friction of about 6 amu/ps, which corresponds to a dynamic friction force $f_{\rm k} = \gamma v$ of about 6 fN/atom at the velocity of $v = 840$ m/s in agreement with the upper bound estimated experimentally.[1] Moreover, our methods and numerical observations show that commensurate and incommensurate DWNTs of equal dimensions can have identical values of the friction coefficient, confirming the results by Tangney et al..[9] For the different DWNTs considered in the present paper, the force of dynamic friction remains linear in the velocity in a significant domain of initial conditions.

Beyond the linear domain, nonlinear effects become important which increase dynamic friction and which depend on the geometry of the DWNTs. For zigzag-armchair and zigzag-zigzag DWNTs, the domain of validity of linear friction extends up to 90% of the complete extraction. However, for armchair-armchair DWNTs, nonlinear effects set in at a smaller fraction of the complete extraction. This fraction decreases with the radii of the armchair-armchair DWNTs. In the nonlinear domain, friction is enhanced because of the excitation of internal modes of the DWNT by a possible mechanism of resonance. These nonlinear effects can be studied by the methods of dynamical systems theory combined with nonequilibrium statistical mechanics.

The dynamics of DWNTs certainly involves other degrees of freedom than the one-dimensional translational motion along the axis of the tubes. Indeed, molecular dynamics simulations display a rich variety of motions, such as the rotation of one tube with respect to the other around the axis of the tubes. Dynamic friction is also associated with this rotational motion which is important for nanobearings and we intend to report on this other friction property in a future publication.

**Acknowledgments.** Part of the computations have been performed with the 32-processor cluster ANIC-2 of the Laboratory of Statistical Physics and Plasmas of ULB. This research is financially supported by the "Communauté française de Belgique" (contract "Actions de Recherche Concertées" No. 04/09-312) and the National Fund for

Scientific Research (F. N. R. S. Belgium, contract F. R. F. C. No. 2.4577.04).

---


[1] J. Cumings and A. Zettl, Science **289**, 602 (2000).
[2] Q. Zheng and Q. Jiang, Phys. Rev. Lett. **88**, 045503 (2002).
[3] Q. Zheng, J. Z. Liu, and Q. Jiang, Phys. Rev. B **65**, 245409 (2002).
[4] S. B. Legoas *et al*, Phys. Rev. Lett. **90**, 055504 (2003).
[5] J. Servantie and P. Gaspard, Phys. Rev. Lett. **91**, 185503 (2003).
[6] J. L. Rivera, C. McCabe, and P. T. Cummings, Nano Lett., **3**, 1001 (2003).
[7] Y. Zhao, C. C. Ma, G. H. Chen, and Q. Jiang, Phys. Rev. Lett. **91**, 175504 (2003).
[8] A. N. Kolmogorov and V. H. Crespi, Phys. Rev. Lett. **85**, 4727 (2000).
[9] P. Tangney, S. G. Louie, and M. L. Cohen, Phys. Rev. Lett. **93**, 065503 (2004).
[10] C. Jarzynski, Phys. Rev. Lett. **71**, 839 (1993).
[11] M. Berry and J. Robbins, Proc. Roy. Soc. Lond. A. **442**, 659 (1993).
[12] D. W. Brenner, Phys. Rev. B **42**, 9458 (1990).
[13] R. Saito, G. Dresselhaus, and M. S. Dresselhaus, *Physical Properties of Carbon Nanotubes* (Imperial College Press, London, 1998).
[14] J.P. Lu, X. P. Li, and R. M. Martin, Phys. Rev. Lett. **68**, 1551 (1992)
[15] A. Buldum and J.P. Lu, Phys. Rev. Lett. **83**, 5050 (1999)
[16] It should be noticed that the Lennard-Jones potential (2) does not taken into account the directionality of the interlayer delocalization of the $\pi$ orbitals[8] and gives an approximation of the interaction between the nanotubes in this regard.
[17] J. Hone, B. Batlogg, Z. Benes, A. T. Johnson, and J. E. Fisher, Science **289**, 1730 (2000).
[18] A. Einstein, Ann. Phys. **17**, 549 (1905).
[19] J. G. Kirkwood, J. Chem. Phys. **14**, 180 (1946).
[20] H. Mori, Prog. Theor. Phys. **33**, 423 (1965).
[21] S. H. Lee and R. Kapral, J. Chem. Phys. **121**, 11163 (2004).
[22] P. Español and I. Zúñiga, J. Chem. Phys. **98**, 574 (1993).
[23] F. Ould-Kaddour and D. Levesque, J. Chem. Phys. **118**, 7888 (2003).
[24] C. C. Ma, Y. Zhao, C. Y. Yam, G. H. Chen, and Q. Jiang, Nanotechnology **16**, 1253 (2005).
[25] R. M. Corless, G. H. Gonnet, D. E. G. Hare, D. J. Jeffrey, and D. E. Knuth, Adv. Comput. Math. **5**, 329 (1996).
[26] R. Kubo, M. Toda, and N. Hashitsume, *Statistical Physics II: Non-equilibrium Statistical Mechanics*, 2nd ed. (Springer, Berlin, 1998).